Astron. Astrophys. 340, 617–625 (1998)

ASTRONOMY AND ASTROPHYSICS

Computations of Comptonized model atmospheres and X-ray spectra: DA white dwarfs HZ 43 and PG 0824+289

J. Madej

Astronomical Observatory, Warsaw University, Al. Ujazdowskie 4, PL-00478 Warszawa, Poland

Received 30 June 1998 / Accepted 10 September 1998

Abstract. This paper presents a new method for the calculation of LTE model atmospheres and their theoretical spectra, under conditions relevant to hot white dwarfs. The new method rigorously takes into account noncoherent (Compton) scattering of isotropic radiation by free electrons. Scattering is described by the Fokker–Planck expansion of the full scattering kernel, valid at $h\nu \ll mc^2$ and $kT \ll mc^2$ (Kompaneets equation). Iterations of a model atmosphere are performed following the Rybicki numerical scheme, supplemented by noncoherent scattering terms.

The constraint of radiative equilibrium has been linearized with respect both to the Planck function and the noncoherent scattering term simultaneously. Such a double linearization yields rapid temperature corrections, particularly in the uppermost scattering dominated layers of a stellar atmosphere.

The code has been used to compute sample series of pure H models at $T_{\rm eff} = 10^5$ K and various $\log g$. The models clearly exhibit the typical effects of Compton scattering in a stellar atmosphere, i.e. the rise of gas temperature in the uppermost, mostly scattering layers, and significant deficiency and flux cutoff in the emerging X-ray spectrum. The paper presents also Comptonized model spectra of two hot hydrogen-rich (DA) white dwarfs: HZ 43 and PG 0824+289, in which the helium number abundance is exceptionally low, $N_{He}/N_H \leq 10^{-7}$. Compton scattering has practically no impact on UV and EUV spectra of both stars as seen by IUE, ROSAT WFC, and EUVE detectors. However, in both stars there exists the predicted decrease of X-ray flux below 50 Å and the cutoff at 40 and 39 Å (0.3 keV), respectively, which is in the range of e.g. ROSAT PSPC and HRI instruments. The effect is restricted to pure hydrogen atmospheres of both stars and vanishes when $N_{He}/N_H > 10^{-3}$.

Compton scattering of X-rays is therefore equivalent to some additional opacity in that spectral region, which appears only in DA white dwarfs. On the other hand, Compton scattering cannot account for the "missing" opacity in EUV and UV spectra of these stars.

Key words: radiative transfer – scattering – stars: atmospheres – stars: white dwarfs

1. Introduction

Electron scattering is an important opacity source in atmospheres of hot stars. An usual approximation to that process is known as Thomson scattering. This is quite a standard approximation, which assumes that the scattering of radiation on free electrons is a fully coherent event, in which the frequency of a photon is kept fixed before and after scattering. Since Thomson scattering is perfectly grey, it does not leave any specific signature in the spectrum of radiation emerging from the star.

The assumption of Thomson scattering causes a very important implication, that there is no energy and momentum exchange during photon–electron collision. One can say, that the properties (temperatures) of radiation and matter are perfectly decoupled in a strongly scattering atmosphere. This is the case of hot stellar atmospheres, in which matter is strongly ionized and then electron scattering dominates the opacity. Thomson scattering does not influence the equation of radiative equilibrium, because scattering terms there precisely cancel out (Mihalas 1978).

Compton scattering is the same physical photon–electron process which is described with a very precise mathematical formulation, in which both photon and electron change their energies and momenta as is required by the conservation principles. A correct mathematical description of Compton scattering from thermal electrons includes the following physical effects: reddening of scattered photons due to electron recoil effect, broadening (in frequency scale) of the incident radiation spectrum due to the chaotic thermal motion of electrons, and the blue shift of the incident photons known as the inverse Compton effect. Moreover, there exists nonzero induced Compton scattering. A full description of Compton scattering is given by Pomraning (1973). In case of $h\nu \ll m_e c^2 = 511$ keV there exists also the Fokker–Planck expansion of scattering integrals referred to as Kompaneets equation (Kompaneets 1957; Rybicki & Lightman 1979). However, derivation of the Kompaneets equation requires at the very beginning that the scattered radiation field is isotropic, whereas Pomraning's equation does not require such an assumption.

Compton scattering opacity remains practically grey in X-ray domain. However, the nonzero exchange of energies between colliding particles implies a coupling between radiation

and matter. Consequently, Compton scattering can influence the temperature structure of a stellar atmosphere. In case that the white dwarf atmosphere contains hydrogen alone, this effect is most significant and appears as a distinct rise of temperature in the outermost layers (Madej 1993, 1994a, 1994b). The heating effect results from scattering of hard radiation from deep and hot layers of thermalization with cooler gas at the external boundary of an atmosphere.

The other problem is the Compton scattering of X-ray photons in atmospheres of hot stars, $T_{\rm eff} \sim 10^5$ K or more. In this case the energy of scattered photons (0.1–1 keV) strongly exceeds thermal energy of electrons ($kT \sim 10$ eV). Therefore $h\nu > 4kT$, and then the effect of electron recoil dominates. Compton scattering of X-rays proceeds with loss of photon energy to the electron pool (Rybicki & Lightman 1979). It causes a redistribution of X-ray photons to lower energies and, consequently, decreases the X-ray flux (cf. Madej 1993, 1994a, 1994b).

A discussion of this spectral feature in still cooler pure hydrogen (DA) white dwarfs is one of the subjects of this paper. Presentation of both Compton scattering effects in atmospheres of hot neutron stars (Type I X-ray bursters) is given by Madej (1991), cf. also London et al. (1986).

1.1. Impact on spectral lines

Scattering by free electrons has to be treated as noncoherent in cases, when the spectrum contains narrow spectral lines. Then the width of a line can get smaller than the electron Doppler width. There exists a series of papers, which investigated the importance of noncoherent continuum scattering for the formation and broadening of spectral lines in the visual and UV spectral region (cf. Rybicki & Hummer 1994 for the reference list).

Generally, such an interaction between electron Doppler frequency shifts and thermally broadened spectral lines can cause observable broadening of lines in spectra of the hottest stars. Recent papers by Hillier (1991) and Hamann et al. (1992) demonstrate the effect in theoretical spectra of Wolf–Rayet stars. Rybicki & Hummer (1994) present a new numerical method for the computations of NLTE populations in presence of noncoherent electron scattering. The authors predict the existence of a whole pattern of spectral effects due to noncoherent electron scattering and claim, that the effect influences the NLTE level populations and therefore both visual and UV continuum lines and spectra of stars with $T_{\rm eff}$ around 50 000 K and low surface gravities.

However, all the above papers investigate noncoherent scattering due solely to thermal motion of free electrons, which is only a single component of the Compton scattering. Effects of photon redshift due to electron recoil and the Doppler blueshift of scattered photons, as well as induced scattering are not considered there. Therefore the above approach cannot be used to investigate Compton heating effects nor the study of continuum X-ray spectra.

1.2. Diffusion equation

There exist quite numerous research papers in which Compton scattering in the diffusion approximation has been included in the radiative transfer. Ross (1979) developed and applied his numerical method to study the radiative transfer in spherical shells around a compact object, being the source of X-rays. A discussion of the Kompaneets equation and the relevant radiative transfer models was extensively presented by Sunyaev & Titarchuk (1980). Also London et al. (1986) applied their computer code to compute a set of theoretical model atmospheres of X-ray burst sources (see Lewin & Joss 1981, 1983; and Joss & Rappaport 1984 for a description of this class of objects).

However, there exists an important limitation of the computer codes based on the diffusion approximation (or Kompaneets equation). As Rybicki & Hummer (1994) point out, the diffusion equation can be used only if the radiation field varies slowly with frequency, i.e. changes of the radiation field are small on the frequency shift after Compton scattering. Therefore the diffusion approximation to Compton scattering is appropriate to the radiative transfer in continua, whereas it is not useful to both LTE and NLTE radiative transfer involving narrow spectral lines.

Such a statement implies also, that unfortunately NLTE model atmosphere computations with Compton scattering have to be ruled out, when using otherwise a physically correct diffusion equation. This is because NLTE model computations can yield physically false conclusions on the NLTE occupation numbers, if line transitions were ignored (Mihalas 1978).

This research follows a series of papers on the treatment of Compton scattering in white dwarfs and X-ray bursters, in which two different numerical methods have been defined and tested already (Madej 1991, 1994b). This paper presents the third numerical technique for that purpose, which is certainly the most realistic and accurate among them. Moreover, the following method can be used as an extension of other algorithms which used coherent Thomson scattering only. This allows one for the investigation of both the continuum X-ray spectra of hot stars, and the effects of Compton heating on the uppermost atmospheric layers. However, narrow spectral lines still cannot be included there, which prevents realistic computations of NLTE effects.

There exists a number of various formulations of the radiative transfer equation including Compton scattering (cf. Pomraning 1973; Rybicki & Lightman 1979), suitable either to classical or to fully relativistic plasmas. The following chapters present a discussion of stellar atmospheres at $T_{\rm eff}$ of the order 10^5 K, and make use of the nonrelativistic diffusion approximation to the Compton scattering following Pomraning (1973). The diffusion equation adopted from Pomraning (1973) is more general than the Kompaneets equation in Rybicki & Lightman (1979), but both are identical in case when the angular distribution of scattered photons is isotropic.

The diffusion equation takes into account all the physical effects present in the scattering process, and is not restricted to the electron Doppler broadening alone. However, further dis-

cussion will be restricted to LTE model atmospheres with no spectral line opacities. This yields only conclusions concerning effects of Compton heating in the uppermost layers and X-ray spectra of the models.

2. Model atmosphere equations

2.1. The equation of radiative transfer

Equations of a model atmosphere with plane-parallel geometry can be written on the geometrical vertical depth z. Since both gas temperature and photon energies are small compared to the electron rest mass, $kT \ll mc^2$ and $h\nu \ll mc^2$, photon diffusion in frequency space due to repeated Compton scatterings can be written in the diffusion approximation. The corresponding equation of radiative transfer was given by Pomraning (1973, Eq. 8.620), and here it reduces to

$$\begin{aligned}\mu\frac{\partial I_\nu}{\partial z} &= \kappa_\nu(B_\nu - I_\nu) - \sigma_T I_\nu + \sigma_T J_\nu \\ &+\sigma_T\left[\frac{kT}{mc^2}\nu^2\frac{\partial^2}{\partial\nu^2} + \left(\frac{h\nu}{mc^2} - 2\frac{kT}{mc^2}\right)\nu\frac{\partial}{\partial\nu}\right. \\ &\left.+\frac{h\nu}{mc^2}\right] J_\nu - \sigma_T\frac{c^2}{h\nu^3}\frac{h\nu}{mc^2}J_\nu\left(1-\nu\frac{\partial}{\partial\nu}\right)J_\nu\,, \quad (2.1)\end{aligned}$$

which is valid for the isotropic distribution of scattered photons. J_ν has the usual meaning of the mean intensity of monochromatic radiation. The absorption coefficient κ_ν (taken for 1 cm^3) includes already stimulated emission. Scattering coefficient σ_T is equal to the classical Thomson value, $\sigma_T = 6.65\times10^{-25}\,n_e$ cm^{-1}, where n_e stands for the number of free electrons in unit volume. Stimulated scattering is represented by the last (quadratic) term in Eq. (2.1).

Eq. (2.1) clearly demonstrates, that the scattering emissivity is represented by a sum of coherent and noncoherent contributions (terms: $+\sigma_T J_\nu$ and that in square brackets, respectively). Noncoherent terms are proportional either to kT/mc^2 or to $h\nu/mc^2$, which are of the order 10^{-5} in atmospheres of hot white dwarfs and in their UV and X-ray spectra. Therefore they represent rather small perturbations in the equation of transfer.

The noncoherent scattering terms in Eq. (2.1) can also be obtained from the widely used Kompaneets diffusion equation (Rybicki & Lightman 1979), if we replace dimensionless variables in that equation by dimensional both frequencies and true/mean intensities of radiation. The equation of transfer, when written on the monochromatic optical depth scale τ_ν at some frequency ν, changes to

$$\begin{aligned}\mu\frac{\partial I_\nu}{\partial\tau_\nu} &= I_\nu - \epsilon_\nu B_\nu - (1-\epsilon_\nu)J_\nu - (1-\epsilon_\nu)\,Y_\nu \\ Y_\nu &= \frac{kT}{mc^2}\nu^2\frac{\partial^2 J_\nu}{\partial\nu^2} + \frac{h\nu-2kT}{mc^2}\nu\frac{\partial J_\nu}{\partial\nu} + \frac{h\nu}{mc^2}J_\nu \\ &-\frac{h\nu}{mc^2}\frac{c^2}{h\nu^3}J_\nu^2 + \frac{h\nu}{mc^2}\frac{c^2}{h\nu^3}J_\nu\cdot\nu\frac{\partial J_\nu}{\partial\nu}\,, \quad (2.2)\end{aligned}$$

where $\epsilon_\nu = \kappa_\nu/(\kappa_\nu+\sigma_T)$. At the effective temperatures corresponding to white dwarfs the Compton scattering term Y_ν is a small correction to the standard equation of transfer with coherent scattering, and it is nonlinear with respect to the radiation mean intensity J_ν. In thermodynamical equilibrium ($J_\nu = B_\nu$), the noncoherent scattering term $Y_\nu = 0$, which can be shown by direct computations.

Following the usual steps in the radiative transfer we can obtain the zeroth and first momenta of the equation of transfer

$$\frac{\partial H_\nu}{\partial\tau_\nu} = \epsilon_\nu(J_\nu - B_\nu) - (1-\epsilon_\nu)\,Y_\nu\,, \quad (2.3)$$

$$\frac{\partial K_\nu}{\partial\tau_\nu} = H_\nu\,, \quad (2.4)$$

Variables J_ν, H_ν, and K_ν denote mean intensity of radiation, monochromatic flux, and the second moment of true intensity I_ν, respectively. Both equations joined together form a single scalar equation of transfer of the second order

$$\frac{\partial^2}{\partial\tau_\nu^2}(f_\nu J_\nu) = \epsilon_\nu(J_\nu - B_\nu) - (1-\epsilon_\nu)\,Y_\nu\,, \quad (2.5)$$

with the variable Eddington factors f_ν closing the transfer problem, $K_\nu = f_\nu J_\nu$. Eq. (2.5) can be solved by iterations (Mihalas 1978). All the following equations include factors f_ν and therefore are exact. However, for numerical convenience, factors f_ν were set to 0.333333 throughout this paper. Consequently, model computations presented in this paper are in fact computed in the Eddington approximation.

The equation of transfer (2.5) can be most conveniently written on the optical depth scale at some fixed (standard) frequency, which then becomes the unique independent variable. Such a standard optical depth will be denoted below by τ with no subscript. The equation of transfer, Eq. (2.5), takes then the form

$$\frac{1}{\eta_\nu}\frac{\partial}{\partial\tau}\left[\frac{1}{\eta_\nu}\frac{\partial}{\partial\tau}(f_\nu J_\nu)\right] = \epsilon_\nu(J_\nu - B_\nu) - (1-\epsilon_\nu)\,Y_\nu\,, \quad (2.6)$$

with the dimensionless variable $\eta_\nu = (\kappa_\nu+\sigma_T)/(\kappa_\nu+\sigma_T)_{std}$.

2.2. Radiative equilibrium and linearization procedure

The equation of radiative equilibrium in a stellar atmosphere requires constancy of the bolometric flux with geometrical depth, $dH/dz = 0$. Following Eq. (2.5) we obtain

$$\int_0^\infty \eta_\nu\epsilon_\nu(J_\nu - B_\nu^*)\,d\nu - \int_0^\infty \eta_\nu(1-\epsilon_\nu)\,Y_\nu^*\,d\nu = 0\,. \quad (2.7)$$

An asterisk attached to the Planck function B_ν^* and the Compton scattering term Y_ν^* denotes, that both of them are computed at the correct temperature distribution $T^*(\tau)$, which yet remains unknown.

We can expand both B_ν^* and Y_ν^* in Taylor series at the actual $T(\tau)$, and neglect higher order terms

$$B_\nu^*(\tau) = B_\nu(\tau) + \left(\frac{\partial B_\nu}{\partial T}\right)_\tau \Delta T(\tau)\,, \quad (2.8)$$

$$Y_\nu^*(\tau) = Y_\nu(\tau) + \left(\frac{\partial Y_\nu}{\partial T}\right)_\tau \Delta T(\tau)\,, \quad (2.9)$$

where $\Delta T = T^* - T$. Substituting to Eq. (2.7) one gets the linearized equation of radiative equilibrium

$$\int_0^\infty \eta_\nu \epsilon_\nu (J_\nu - B_\nu)\, d\nu - \int_0^\infty \eta_\nu (1-\epsilon_\nu)\, Y_\nu\, d\nu \qquad (2.10)$$
$$= \Delta T \left\{ \int_0^\infty \eta_\nu \epsilon_\nu \frac{\partial B_\nu}{\partial T}\, d\nu + \int_0^\infty \eta_\nu (1-\epsilon_\nu)\, \frac{\partial Y_\nu}{\partial T}\, d\nu \right\},$$

where

$$\frac{\partial Y_\nu}{\partial T} = \frac{k}{mc^2}\nu^2 \frac{\partial^2 J_\nu}{\partial \nu^2} - \frac{2k}{mc^2}\nu \frac{\partial J_\nu}{\partial \nu}\,. \qquad (2.11)$$

The correct equation of the radiative transfer is given by Eq. (2.7) with both thermal and Compton scattering terms including B_ν^* and Y_ν^*, in which unknown temperature corrections are already included in computing of the radiation field. Such a widely employed strategy with Y_ν^* term being ignored, ensured fast convergence of $T(\tau)$ to the required values at the radiative equilibrium in both LTE and NLTE model atmospheres (cf. Mihalas 1978). Eq. (2.6) changes then to

$$\frac{1}{\eta_\nu}\frac{\partial}{\partial \tau}\left[\frac{1}{\eta_\nu}\frac{\partial}{\partial \tau}(f_\nu J_\nu)\right]$$
$$= \epsilon_\nu (J_\nu - B_\nu) - (1-\epsilon_\nu)\, Y_\nu$$
$$- \left[\epsilon_\nu \frac{\partial B_\nu}{\partial T} + (1-\epsilon_\nu)\, \frac{\partial Y_\nu}{\partial T} \right] \Delta T\,, \qquad (2.12)$$

where

$$\Delta T = \frac{1}{M} \int_0^\infty \eta_{\nu'} \left[\epsilon_{\nu'} (J_{\nu'} - B_{\nu'}) - (1-\epsilon_{\nu'})\, Y_{\nu'} \right] d\nu'\,, \qquad (2.13)$$

and

$$M = \int_0^\infty \eta_{\nu'} \epsilon_{\nu'} \frac{\partial B_{\nu'}}{\partial T}\, d\nu' + \int_0^\infty \eta_{\nu'} (1-\epsilon_{\nu'})\, \frac{\partial Y_{\nu'}}{\partial T}\, d\nu'\,. \qquad (2.14)$$

The right-hand side of the equation of transfer is a complex nonlinear expression with respect to the unknown variable J_ν.

2.3. Discretization and iterations

Computations of model stellar atmosphere are routinely performed with grids of discrete points, which replace integrals and differentials by quadrature sums and finite differences. The equation of transfer with continuum variables, Eq. (2.12), is then transformed to the following grids: standard optical depths $\{\tau_d\}$, $d = 1, \ldots, D$, and discrete frequencies $\{\nu_i\}$, $i = 1, \ldots, I$.

Representation of the differential operator in Eq. (2.12) is a standard problem and will not be discussed below. Discretization of the right-hand side of the equation of transfer yields the following algebraic equation at the depth τ_d and frequency ν_i

$$\left\{ \frac{1}{\eta_i}\frac{\partial}{\partial \tau}\left[\frac{1}{\eta_i}\frac{\partial (f_i J_i)}{\partial \tau}\right] \right\}_d$$
$$= \epsilon_i (J_i - B_i) - (1-\epsilon_i)\, \tilde{Y}_i$$
$$- \left[\epsilon_i \frac{\partial B_i}{\partial T} + (1-\epsilon_i)\, \frac{\partial \tilde{Y}_i}{\partial T} \right] \Delta T\,, \qquad (2.15)$$

where

$$\Delta T = \frac{\sum_{k=1}^{I} w_k \eta_k \left[\epsilon_k (J_k - B_k) - (1-\epsilon_k)\, \tilde{Y}_k \right]}{\sum_{k=1}^{I} w_k \eta_k \epsilon_k\, (\partial B_k/\partial T) + \sum_{k=1}^{I} w_k \eta_k (1-\epsilon_k)\, \partial \tilde{Y}_k/\partial T}\,. \qquad (2.16)$$

Values of w_k denote the quadrature weights for frequency integration.

Eqs. (2.15) and (2.16) describe the radiation field on the intermediate optical depths, i.e. at the levels $d = 2, \ldots, D-1$. Compton scattering terms Y_i are adorned here with tilde sign, which indicates that they are computed on the basis of the radiation field found in the previous iteration (see also an explanation below). Both boundary conditions at $d = 1$ and $d = D$ can also be expressed by relevant algebraic expressions (see Madej 1994b).

At any single frequency ν_i and optical depth τ_d, the equation of transfer (2.15) involves the whole spectrum of radiation hidden in temperature corrections ΔT. In case if strictly coherent Thomson scattering terms are included ($\tilde{Y}_\nu = 0$), there exist a number of numerical methods well suited to handle problems of LTE and NLTE model atmosphere computations. A very useful and stable technique for model atmosphere computations (with step-by-step eliminations of numerous frequency points) can be derived from Rybicki's "grand matrix" formulation (Rybicki 1971, Mihalas 1978).

The presence of nonzero Compton terms involves frequency derivatives of the radiation mean intensity J_ν, and this very seriously complicates the overall elimination scheme. A numerical technique for model atmosphere computations with Compton scattering, the elimination scheme, and the set of sample models has been presented by Madej (1994b). However, accuracy and convergence properties of that method still require additional improvements. Moreover, that algorithm is a very specific construction and cannot be used to upgrade existing codes written by other authors using a variety of techniques.

This paper proposes a simple iterative approach to solve the above model atmosphere equations. At the first iteration one starts with a roughly guessed temperature stratification $T(\tau)$, where the computer solves the LTE equation of state and finds monochromatic opacities at each frequency and depth point, ν_i and τ_d, respectively. Then the radiation field is found by a repeated solution of the radiative transfer equation, Eq. (2.15), in which $\tilde{Y}_i$, $\partial \tilde{Y}_i/\partial T$, and ΔT were set to zero. I.e. this represents a standard coherent scattering problem. After that iteration, tables of both $\partial^2 J_\nu/\partial \nu^2$ and $\partial J_\nu/\partial \nu$ were determined, yielding the initial temperature corrections ΔT in the model, according to Eq. (2.16). The ΔT's include already Compton scattering terms.

The second and all the remaining iterations solve the full radiative transfer equation, Eq. (2.15) with a nonzero ΔT. However, terms $\tilde{Y}_i$ and $\partial \tilde{Y}_i/\partial T$ are taken from the previous iteration.

Therefore all subsequent iterations solve the standard model atmosphere problem, in which the new radiation field is computed as in the Thomson scattering case. The only difference is that new Compton scattering terms are computed on the basis of the radiation field from the previous iteration, and are appended either to the inhomogeneous thermal term ($\epsilon_\nu B_\nu$), or to the $\triangle T$ term in the current iteration.

In other words, such a scheme makes computing of the Comptonized model generally very similar to the classical computations with coherent Thomson scattering. Noncoherent scattering terms are iterated by a lambda-iteration, whereas the remaining part of the problem was iterated with the efficient Rybicki method. Such applied lambda-iterations yield radiative equilibrium in a Comptonized atmosphere very promptly. Fast convergence of temperature corrections $\triangle T$ to the values reflecting Compton heating in the uppermost layers of a model is not surprising, since that heating is restricted to layers of very small optical depth (cf. the following sections). The presence of noncoherent scattering terms practically does not increase the computing time of the new algorithm, as compared with the original coherent scattering code.

2.4. Extending of Thomson scattering codes

The above Compton scattering algorithm represents a quite simple overlay, which can be joined with any particular Thomson scattering model atmosphere code, which includes already $\triangle T$ corrections in the equation of transfer (Mihalas 1978). Addition of Compton scattering terms essentially does not influence the structure of the host code. The only two necessary interface adjustements extend the expression for $\triangle T$, Eq. (2.16), and extend also the expression for the scaling coefficient

$$\epsilon_i \frac{\partial B_i}{\partial T} \quad \rightarrow \quad \epsilon_i \frac{\partial B_i}{\partial T} + (1-\epsilon_i)\,\frac{\partial \tilde{Y}_i}{\partial T}\,, \tag{2.17}$$

appearing on the right hand side of the equation of transfer, Eq. (2.15). The coefficient $\epsilon_i(\partial B_i/\partial T)$ appears normally in other model atmosphere codes (both LTE and NLTE), in which Thomson scattering was assumed and then thermal terms only contributed to the temperature corrections included in the equation of radiative transfer (Mihalas 1978).

The overall accuracy of the final computer code strongly depends on a very accurate representation of the partial derivatives $\partial J_\nu/\partial\nu$ and $\partial^2 J_\nu/\partial\nu^2$, and consequently $\tilde{Y}_\nu$ and $\partial\tilde{Y}_\nu/\partial T$. In this research a second-order difference representation is used for $\partial^2 J_\nu/\partial\nu^2$, and $\partial J_\nu/\partial\nu$ is the first derivative of the Lagrange interpolation polynomial of the third degree connecting groups of neighbouring J_i points.

3. Convergence: sample high temperature models

Compton scattering causes two distinct effects in hot stellar atmospheres and in their spectra. First, energy exchange between electron gas and energetic photons coming from deep layers causes an increase of gas temperature in the outermost (mostly scattering) layers of a stellar atmosphere. Second, hard energy photons which lose their energy in the first process are then redistributed to lower frequencies, and this causes a depression of the monochromatic flux of radiation emerging from the atmosphere. The existence of both effects in hot DA white dwarfs was demonstrated in earlier papers with two earlier (independent) computer programs (Madej 1993, 1994a, 1994b).

Both the above effects are caused by Compton scattering of the most energetic photons available in the radiation spectrum, which have energies significantly higher than the average thermal energy of a gas. At the $T_{\rm eff}$'s corresponding to hot white dwarfs both effects are rather marginal as long as the overall spectrum and radiative equilibrium is considered. However, they can be important for the X-ray spectra and the temperature structure in or above line-forming region in the hot atmosphere.

3.1. Pure H models at $T_{\rm eff} = 1 \times 10^5$ K

The overall quality and convergence properties of the new computer code have been tested in a series of LTE model stellar atmospheres computed at $T_{\rm eff} = 1 \times 10^5$ K and various surface gravities, corresponding either to gravities of white dwarfs or subdwarf O stars. The chemical composition of the models included hydrogen only.

All the model atmospheres discussed in this paper were computed over a large range of the standard optical depths, ranging from $\log\tau = -8.0$ to $+3.0$ or even $+4.0$, depending on the model. The number of depth points D approached 130–140, with 12 points per decade. The number of frequency points I always extended 850. Such a choice of model parameters allowed for the reproduction of radiative equilibrium with the accuracy of $\triangle F_{bol}/F_{bol}$ better than 3×10^{-3} in 6–8 iterations, starting from a rough "grey" temperature stratification. However, the convergence of $\triangle T$ was apparently fastest in the highest layers, where Compton scattering dominated absorption by many orders of magnitude.

Fig. 1 displays the run of temperature T vs. the Rosseland optical depth τ_R in a family of pure hydrogen, LTE model atmospheres. Dashed and dotted lines in the Figure present models with $\log g = 8.0$, 6.0, and 5.5, respectively. In all the models Compton scattering produces a characteristic increase of temperature T in the uppermost layers. Note, that the model with $\log g = 8.0$, which is the gravity typical of white dwarfs, exhibits rather remnant Compton heating effect even at the uppermost $\log\tau_R = -8.0$. In the models of lower $\log g$ the effect extends to deeper layers of the atmosphere, still it does not extend deeper than to $\log\tau_R = -5.0$.

The solid line in Fig. 1 presents the run of temperature in the LTE model at $\log g = 8.0$, in which the standard Thomson scattering was assumed. The heating effect obviously is absent in the Thomson scattering model.

Fig. 2 presents synthetic continuum spectra of two models, both with a low surface gravity $\log g = 6.0$. The solid line is the spectrum which includes Compton scattering, whereas the dashed line represents the spectrum of a model atmosphere computed with the standard Thomson scattering. Both spectra are practically identical except for the X-ray branches (at $\lambda < 50$ Å,

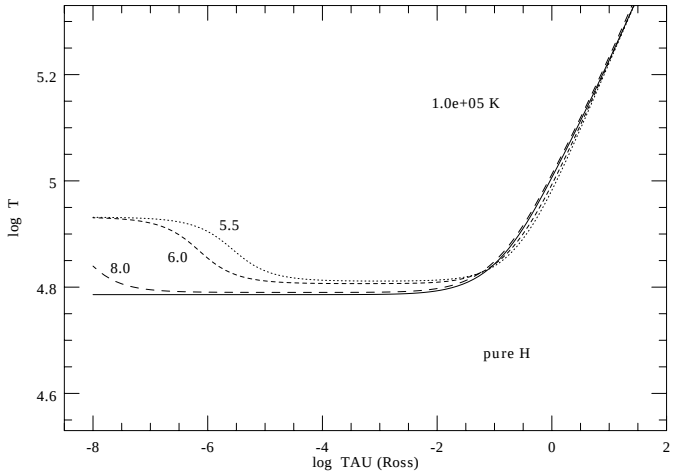

Fig. 1. Run of gas temperature T vs. Rosseland optical depth τ_R in pure H models, computed with account of Compton scattering at $T_{\rm eff} = 10^5$ K and various $\log g$. Effects of Compton heating and cooling by free-free absorption are well pronounced in all the models. Compton heating reaches the maximum extent in model of the lowest gravity, $\log g = 5.5$. For comparison, the solid line presents the run of $T(\tau_R)$ in the model $\log g = 8.0$ computed with coherent Thomson scattering.

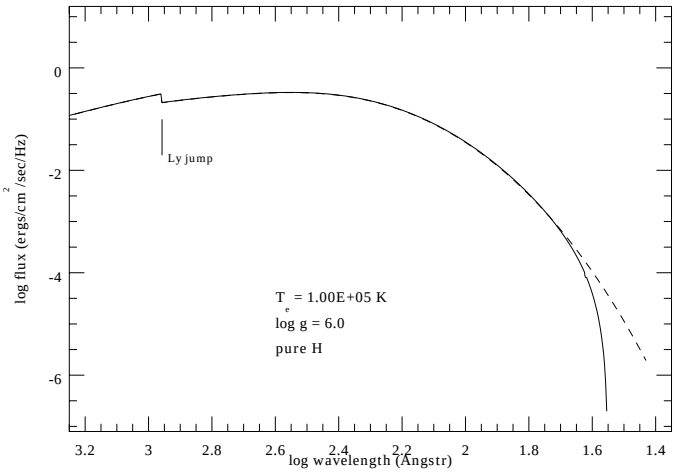

Fig. 2. Spectra of sample pure hydrogen model atmospheres with $T_{\rm eff} = 10^5$ K and $\log g = 6.0$. Solid line represents the spectrum of the atmosphere which includes effects of Compton scattering. Dashed line represents the spectrum of the model which assumes coherent Thomson scattering. Note the depression of flux at $\lambda < 50$ Å and the cutoff at ≈ 36 Å, which illustrate the fact that Compton scattering flushes out hard X-ray photons to longer wavelengths.

i.e. at $h\nu > 0.24$ keV), where one can note a distinct depression of the flux in Comptonized atmosphere, and an apparent cutoff of the flux at ≈ 36 Å (0.33 keV).

The deficiency of X-ray flux in the Comptonized model reflects in fact the difference between photon energies (higher than 400 eV) and the mean thermal energy of scattering electrons (of the order of 10 eV). In this case repeated Compton scatterings cause systematic loss of photon energy and shifts them to longer wavelengths. However, Compton scattering does influence neither visual/UV nor far EUV continuum spectra of the discussed model.

3.2. Influence of heavier elements

Chemical composition of the models included hydrogen alone, since pure hydrogen atmospheres exhibit the most evident effects of Compton scattering. This is due to the fact, that both hydrogen b-f absorption and free-free opacity quickly vanish with increasing frequency ν. Therefore in pure H atmospheres outgoing radiation from the hard-energy branch of the spectrum has been created by thermal processes in particularly deep and hot layers of thermalization. Photons escaping into empty space undergo then numerous Compton scatterings, in which they efficiently lose their energy to cooler electron gas and simultaneously move in the frequency space to lower energies.

In case that helium or heavier elements are present, efficient b-f absorption continua cover the high-energy tails of stellar spectra which moves the thermalization depth upward, just slightly below the stellar photosphere. In such case the significance of Compton scattering very seriously decreases, and both effects (temperature rise and deficiency of X-ray photons) do not develop.

3.3. The Compton y parameter

The Compton y parameter denotes the relative value of energy change which a photon experiences after repeated Compton scatterings in a gas. Rybicki & Lightman (1979) compute y as the product of mean energy change after a single Compton scattering times the number of such events. If the value of y is of the order unity of larger, than the Compton scattering can be generally considered as the dominant agent in the radiative transfer in some medium.

Rybicki & Lightman (1979) derive the following expression describing the relative energy transfer per single scattering, for a photon of initial energy $h\nu$

$$\frac{\Delta h\nu}{h\nu} = \frac{4kT - h\nu}{mc^2} \,. \tag{3.1}$$

The expression is valid for nonrelativistic electrons in thermal equilibrium. For photons penetrating a purely scattering finite layer this yields the approximate expression

$$y = \frac{4kT - h\nu}{mc^2}\ \max\left(\tau_T, \tau_T^2\right) \tag{3.2}$$

where τ_T denotes the total optical depth of the medium with respect to Thomson scattering. Eq. (3.2) is the expected change of energy only for photons of initial energy $h\nu$, and not for the general pool of incident photons.

In a stellar atmosphere of infinite optical depth τ_T has the meaning of the scattering optical depth of the layer, where emerging photons were created by thermal processes (at the depth of thermalization). Thermalization of radiation occurs in a layer of the effective optical depth τ_ν^* of the order unity (cf. also Rybicki & Lightman, 1979, for the definition of the effective optical depth). The value of $\tau_\nu^* = 1$ has been assumed as the

depth of thermalization in the following considerations. Since the free-free absorption (dominating in X-rays in pure H atmosphere) changes as ν^{-3}, the depth of thermalization, τ_T, and the Compton parameter $y(\nu)$ are strongly frequency-dependent quantities.

The useful prescription for computing of τ_T in a real inhomogeneous stellar atmosphere follows from the incremental definitions

$$d\tau_T \;=\; -\sigma_T \rho dz\,, \tag{3.3}$$

$$d\tau^*_\nu \;=\; -\left[\kappa_\nu(\kappa_\nu+\sigma_T)\right]^{1/2}\;\rho dz\,, \tag{3.4}$$

which yields

$$d\tau_T = \left[\kappa_\nu(\kappa_\nu+\sigma_T)\right]^{-1/2}\sigma_T\, d\tau^*_\nu\,, \tag{3.5}$$

We can then integrate Eq. (3.5) to obtain

$$\tau_T(\nu) = \int\limits_0^1 \left(\frac{\sigma_T/\kappa_\nu}{1+\kappa_\nu/\sigma_T}\right)^{1/2} d\tau^*_\nu\,, \tag{3.6}$$

which can be easily computed given the run of monochromatic opacities in a model atmosphere interpolated to the effective optical depth τ^*_ν at the frequency ν. Substituting τ_T to Eq. (3.2) yields the final value of the Compton parameter $y(\nu)$.

In case of the pure H model of $T_{\rm eff} = 10^5$ K and $\log g = 6.0$, the above procedure yields $y(\nu) = -1.10$ at the cutoff $\lambda = 36$ Å. This is a crude estimate which shows, that such photons get substantially redistributed to longer wavelengths when travelling from the layer of thermalization outwards and vanish from that energy range.

4. HZ 43

The binary system HZ 43 is a very bright extrasolar source of radiation in the extreme UV and soft X-rays. Continuum hard photons of the system are radiated by the hot hydrogen-dominated white dwarf, designated as HZ 43 A. Effective temperature and other parameters of the white dwarf were analysed in a number of papers (Paerels et al. 1986, Holberg et al. 1986, Finley et al. 1990, cf. also Barstow et al. 1995a). In this paper I shall adopt results of the recent analysis by Napiwotzki et al. (1993), who derived $T_{\rm eff} = 49\,000$ K and $\log g = 7.7$, based on the archival EXOSAT and ROSAT PSPC data, blue and red visual spectrograms, and the NLTE model atmospheres computed with the code by Werner (1986).

The secondary companion star (HZ 43 B) is classified as a dM3.5e star (Margon et al. 1976). Napiwotzki et al. (1993) presented a thorough spectral analysis of this star and concluded, that the cool component of the HZ 43 system should not contribute to the total EUV and X-ray luminosity at energies above 0.1 keV.

The papers quoted above point out, that the atmosphere of HZ 43 A consists of exceptionally pure H with practically no trace of helium or heavier elements. The NLTE model atmosphere analysis by Napiwotzki et al. (1993) gives only upper limits for abundances of heavier elements. The authors claim,

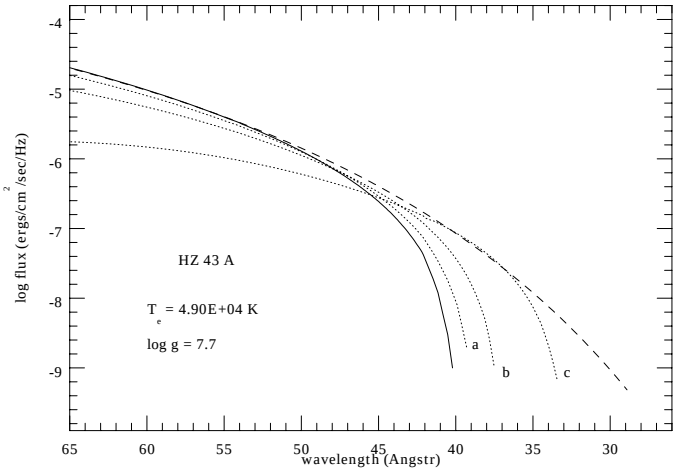

Fig. 3. X-ray spectra of various model atmospheres of the DA white dwarf HZ 43 A. Solid line is the Comptonized spectrum of a pure H model, whereas the dashed line is the Thomson scattering spectrum. Note the X-ray flux deficiency of the spectrum computed with Compton scattering. Dotted lines present Comptonized spectra of H-dominated atmospheres with He number abundance $N_{He}/N_H = 10^{-4}$ (line a), 3×10^{-4} (line b), and 10^{-3} (line c), and with zero abundance of heavier elements.

that the number abundance of helium in HZ 43 A is less than 1.5×10^{-5}. Abundances of CNO elements are even lower, in which the highest is the upper limit of carbon abundance, $N_C/N_H < 3 \times 10^{-6}$. Most recent EUVE observations by Barstow et al. (1995b) yield $N_{He}/N_H < 10^{-7}$.

The pure H model atmosphere of HZ 43 A exhibits an insignificant effect of Compton heating in the uppermost layers, which is related to the lower $T_{\rm eff}$ of this star and rather high gravity (compare to $T(\tau_R)$ curves in Fig. 1). The only clear effect of Comptonisation can be seen in the X-ray spectrum. Fig. 3 displays the X-ray part of its spectrum (solid line), which features a cutoff at $\lambda \approx 40$ Å (0.3 keV). The spectrum of this star computed with account of coherent Thomson scattering (long-dashed line) predicts much higher flux at wavelengths $\lambda < 50$ Å.

The effect can be found in hydrogen-dominated atmospheres only and its existence strongly depends on the remnant abundance of heavier elements. This is illustrated by a set of models, in which small amounts of helium have been added to hydrogen (dotted lines in Fig. 3). The three lines represent X-ray spectra of hydrogen-dominated model atmospheres with $T_{\rm eff}$ and $\log g$ as in HZ 43 A, with the helium number abundance $N_{He}/N_H = 10^{-4}$ (line labeled a), 3×10^{-3} (line b), and 10^{-3} (line c). It is evident, that even small amounts of helium efficiently increase absorption in that spectral region, which in turn reduces the significance of electron scattering. Therefore the value of the Compton parameter y is then reduced in X-rays and the effects of Comptonisation (depression of X-ray flux) quickly vanish.

The real X-ray spectrum of HZ 43 A is best represented by the solid line in Fig. 3, taking into account exceptionally low $N_{He}/N_H \le 10^{-7}$ (Barstow et al. 1995b) and the apparent absence of heavier elements. This is the theoretical predic-

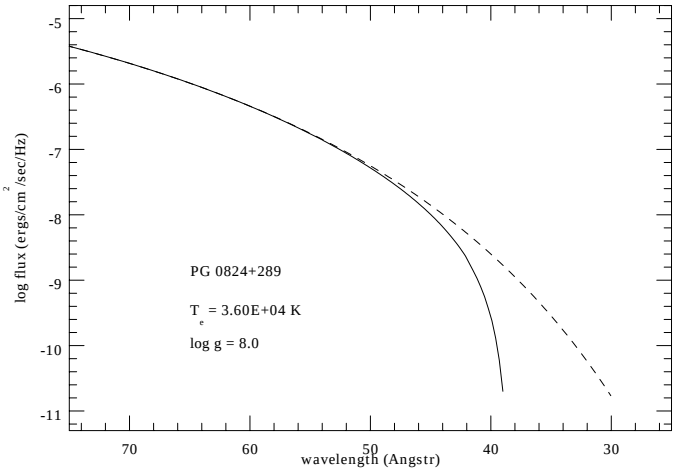

Fig. 4. Same as in Fig. 3 for the DA white dwarf PG 0824+289. Spectra of pure H models only are indicated in the Figure.

tion which at present cannot be verified by observations due to limited spectral resolution of X-ray observations (e.g. that of ROSAT PSPC).

5. PG 0824+289

This star is a spectroscopic binary (hot DA plus dwarf carbon star) accompanied by a visually separated M3-4 dwarf (Heber et al. 1993, Green & Margon 1994). The DA white dwarf belongs to the sample recently analysed by Wolff et al. (1995) on the basis of ROSAT spectral data. A model atmosphere analysis of available spectral observations yielded $T_{\rm eff} = 36\,000$ K at the assumed $\log g = 8.0$, with the estimated error $\triangle T_{\rm eff}$ of several thousands K. The model atmosphere analysis was performed with pure hydrogen LTE models (Koester et al. 1979). Following a brief discussion Wolff et al. (1995) concluded, that the pure H atmosphere of the DA white dwarf satisfactorily represents the X-ray flux of PG 0824+289, and that both the dC and the dM dwarfs do not contribute to the X-ray luminosity of the whole system.

Model atmosphere computations with Compton scattering did not produce any significant $T(\tau_R)$ rise at the outer boundary, and significant effects of noncoherent scattering appear in the X-ray spectrum alone. Fig. 4. displays X-ray branch of the theoretical Comptonized spectrum of PG 0824+289 (solid line). The continuum flux exhibits a cutoff at $\lambda \approx 39$ Å (0.3 keV), and a deficiency of flux at $39\,\text{Å} < \lambda < 50\,\text{Å}$ as compared to the Thomson scattering model (long-dashed line). The effect of flux depression and cutoff in X-ray domain is very similar to that in HZ 43 A.

The value of $y(\nu)$ equals to -0.10 at the cutoff $\lambda = 39$ Å. This value is also similar to that in HZ 43 at the corresponding cutoff.

6. ROSAT PSPC response to theoretical X-ray spectra

The ROSAT Position Sensitive Proportional Counter has a rather poor spectral resolution, which can be roughly approximated by

$$\frac{\triangle E}{E} = 0.43 \left(\frac{E}{0.93} \right)^{-1/2} , \qquad (6.1)$$

where both the true energy E of the photon incident on the PSPC and its measured energy $E + \triangle E$ are expressed in keV. The equation gives the full width at half maximum of a profile describing the scatter of energy measurements. Eq. (6.1) has been given in the Appendix F to the NASA Research Announcements, describing the ROSAT Guest Observer Program.

Theoretical X-ray spectra of both HZ 43 A and PG 0824+289, presented in the previous Sections, can easily be transformed to the shapes as if they were observed with the PSPC detector of a limited spectral resolution. After folding of true spectra with a normalized rectangular profile of width given by Eq. (6.1), the simulated observed spectra approach those obtained with classical Thomson scattering and the flux cutoff shifts to higher energies (0.7 keV, equivalent to 18 Å). There are practically no X-ray photons of such high energies, recorded by ROSAT from both white dwarfs. Therefore one can conclude, that the ROSAT PSPC archival data cannot be analysed to look for the observational confirmation of the energy cutoff in any of the two DA white dwarfs.

7. Summary and conclusions

This paper presents the set of equations which define a LTE model atmosphere in radiative equilibrium with account of Compton scattering. Scattering is described in the diffusion approximation. Full contribution of Compton scattering to the equation of radiative transfer clearly splits into the coherent (Thomson) scattering part and the small noncoherent scattering term.

The corresponding computer code solves the equation of transfer which includes explicitly temperature corrections. Iterations of a model atmosphere are performed following the Rybicki numerical scheme, in which coherent scattering terms alone are directly taken into account in the linearized radiative transfer equation. Noncoherent terms are included here as inhomogeneities. Iterations of a model atmosphere converge very quickly, particularly in the uppermost layers in which continuum scattering exceeds absorption by many orders of magnitude. This occurs because the equation of radiative equilibrium was linearized with respect both to absorption and Compton scattering terms. Numerical tests showed also, that inclusion of Compton scattering in the model equations causes an only very small increase of the computer cpu time, as compared with the cpu time necessary to run the Thomson scattering code.

In other words, the presence of strong Compton scattering helps to restore the radiative equilibrium and fix the right run of temperature with the doubly linearized code. This can occur since Compton scattering causes a nonzero effect on the local temperature, and it is explicitly included in the radiative transfer and the radiative equilibrium equations. On the other hand,

coherent Thomson scattering represents a perfect decoupling between radiation and matter, which is the reason of very serious convergence problems. This topic was extensively discussed e.g. by Mihalas (1978).

The new computer code has been used to calculate sample model atmospheres and continuum spectra of hot, hydrogen dominated white dwarf atmospheres. In case of pure H atmospheres of $T_{\rm eff} = 10^5$ K and various gravities $\log g$, effects of Compton scattering appear distinctly in two ways. First, they cause a rise of electron temperature in the uppermost layers, due to Compton heating of electron gas by hard radiation from below the photosphere. The effect is still rather marginal at $\log g = 8.0$, roughly corresponding to the real white dwarfs, and increases at lower $\log g$. Second, Comptonized spectra exhibit a deficiency of X-ray flux and a subsequent cutoff below 50 Å. This effect occurs at all investigated $\log g$.

In the case of pure H or H dominated atmospheres of HZ 43 and PG 0824+289, no significant heating effect was found there. However, both white dwarfs are predicted to exhibit a deficiency of X-ray flux below 50 Å and the cutoff at 40 and 39 Å, respectively, which is in the range of the ROSAT PSPC and HRI instruments. The presence and exact position of the X-ray cutoff in both stars is the intrisic property of a hydrogen dominated stellar atmosphere, and it vanishes when He number abundance, N_{He}/N_H, rises above 10^{-3}. Compton scattering of X-rays is therefore equivalent to some additional opacity in that spectral region, which appears only in DA white dwarfs with very little or no amounts of heavier elements in their atmospheres.

Additional model computations showed also, that the effects of Compton scattering vanish in mixed H/He or pure He model atmospheres, at least at $T_{\rm eff}$ below 150 000 K. In all the models tested up to now, including pure H atmospheres, these effects do not influence neither IUE, ROSAT WFC, nor EUVE detectors. Therefore Compton scattering cannot account for any "missing" opacity which is sometimes observed in spectra of DA white dwarf stars in the X-ray spectral window.

Acknowledgements. I am very grateful to Dr. K. Werner, the referee, for his comments and corrections to the original version of this paper. This research has been supported by grant No. 2 P03D 013 14 from the Polish Committee for Scientific Research.

References

Barstow, M.A., Holberg, J.B., Koester, D., Nousek, J.A., & Werner, K., 1995a, Proc. of the 9th European Workshop on White Dwarfs, Kiel, Germany, August 1994, eds. D. Koester and K. Werner (Springer Verlag) 302
Barstow M.A., Holberg, J.B., Koester, D., 1995b, MNRAS 274, L31
Finley, D.S., Basri, G., Bowyer, S., 1990, ApJ 359, 483
Green, R.F., Margon, B., 1994, ApJ 423, 723
Hamann, W.-R., Leuenhagen, U., Koesterke, L., Wessolowski, U., 1992, A&A 255, 200
Heber, U., Bade, N., Jordan, S., Voges, W., 1993, A&A 267, L31
Hillier, D.J., 1991, A&A 247, 455
Holberg, J.B., Wesemael, F., & Basile, J., 1986, ApJ 306, 629
Jordan, S., Wolff, B., Koester, D., Napiwotzki, R., 1994, A&A 290, 834
Joss, P.C., & Rappaport, S.A., 1984, ARA&A 22, 537
Koester, D., Schulz, H., Weidemann, V., 1979, A&A 76, 262
Kompaneets, A.S., 1957, Sov. Phys. JETP 4, 730
Lewin, W.H.G., Joss, P.C., 1981, Space Sci. Rev. 28, 3
Lewin, W.H.G., Joss, P.C., 1983, in *Accretion–driven Stellar X-ray Sources*, ed. W.H.G. Lewin and E.P.J. van den Heuvel (Cambridge University Press), 41
Liebert, J., Bergeron, P., Tweedy, R.W., 1994, ApJ 424, 817
London, R.A., Taam, R.E., Howard, W.M., 1986, ApJ 306, 170
Madej, J., 1991, ApJ 376, 161
Madej, J., 1993, in White Dwarfs: Advances in Observation and Theory. NATO ASI Ser., ed. M.A. Barstow (Dordrecht: Kluwer), 273
Madej, J., 1994a, A&A 286, 515
Madej, J., 1994b, Acta Astr. 44, 191
Margon, B., Liebert, J., Gatewood, G., Lampton M., Spinrad H. Bowyer S., 1976, ApJ 209, 525
Mihalas, D., 1978, Stellar Atmospheres, Freeman, San Francisco
Napiwotzki, R., Barstow, M., Fleming, T., Holweger, H., Jordan, S., Werner, K., 1993, A&A 278, 478
Pomraning, G.C., 1973, The equations of radiation hydrodynamics, Pergamon Press
Paerels, F.B.S., Bleeker, A.M., Brinkman, A.C., Gronenschild, E.H.B.M., Heise, J., 1986, ApJ 308, 190
Ross, R.R., 1979, ApJ 233, 334
Rybicki, G., 1971, JQSRT 11, 589
Rybicki, G.B, Hummer, D.G., 1994, A&A 290, 553
Rybicki, G.B., Lightman, A.P., 1979, Radiative Processe in Astrophysics, Wiley, New York
Sunyaev, R.A., & Titarchuk, L., 1980, A&A 86, 121.
Werner, K., 1986, A&A 161, 177.
Wolff, B., Jordan, S., Bade, N., Reimers, D., 1995, A&A 294, 183.